

# Optimizing the Surface Texture and Chemistry of Laser Powder Bed Fusion (LPBF) Haynes 282 for Increased Solar Absorptance

*Junwon Seo<sup>1</sup>, Andrea Ambrosini<sup>2</sup>, Erfan Rasouli<sup>3</sup>,  
Ansel Blumenthal<sup>2</sup>, Vinod Narayanan<sup>3</sup>, Anthony Rollett<sup>1</sup>*

<sup>1</sup>Materials Science and Engineering, Carnegie Mellon University, Pittsburgh, PA, USA

<sup>2</sup>Concentrating Solar Technologies, Sandia National Laboratories, Albuquerque, NM, USA

<sup>3</sup>Mechanical and Aerospace Engineering, University of California, Davis, CA, USA



# Agenda

- Motivation
- Experiments
- Results & Discussion
- Conclusions



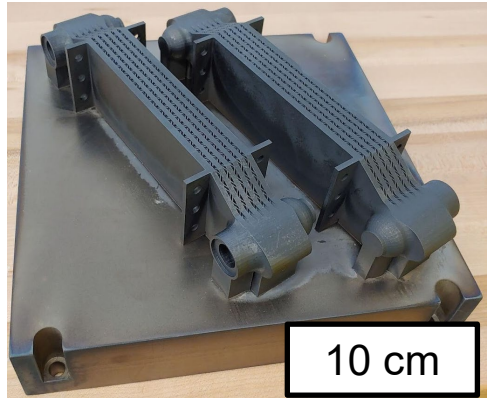
Motivation

# THE SURFACE OF LPBF AM PARTS



# LPBF allows us to print complex geometries with a high surface-to-volume ratio.

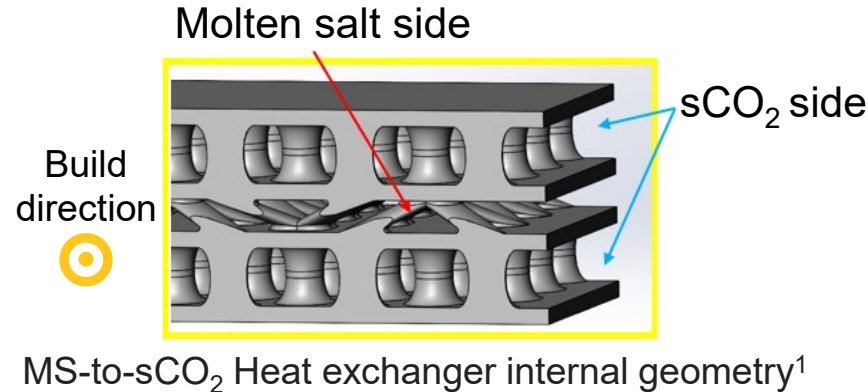
How much control do we have over the surface during printing?



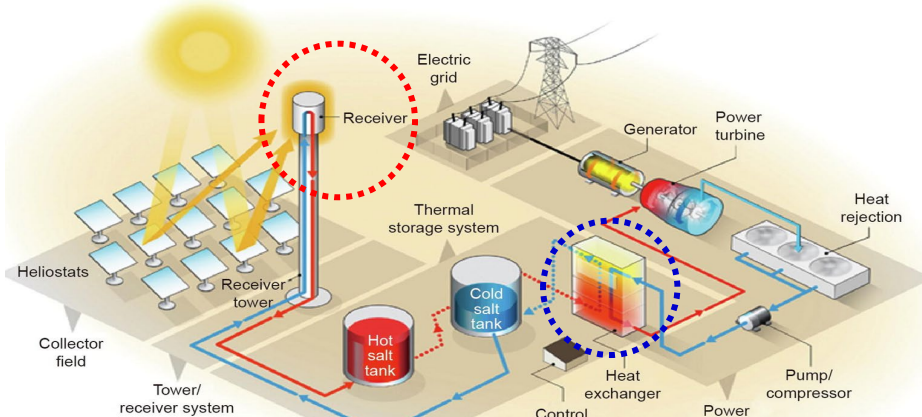
Haynes 282 MS-to-sCO<sub>2</sub> heat exchangers



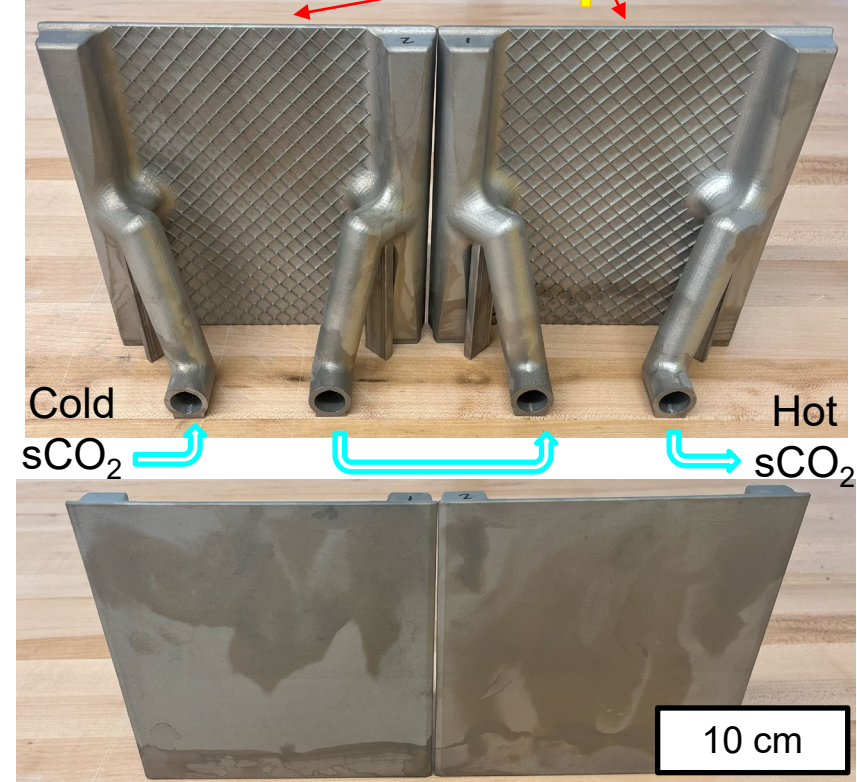
Haynes 282 stand-alone modular counter flow heat exchanger



MS-to-sCO<sub>2</sub> Heat exchanger internal geometry<sup>1</sup>



CSP power generation<sup>2</sup>



Haynes 282 sCO<sub>2</sub> solar receivers



SOLAR ENERGY  
TECHNOLOGIES OFFICE  
U.S. Department Of Energy



<sup>1</sup>Tano, I.N., Rasouli, E., Ziev, T., Seo, J., Lamprinakos, N., Vaishnav, P., Rollett, A., Wu, Z. and Narayanan, V., 2022, July. In *Energy Sustainability* (Vol. 85772, p. V001T05A005). American Society of Mechanical Engineers.

<sup>2</sup>Ding, Wenjin, and Thomas Bauer. "Progress in research and development of molten chloride salt technology for next generation concentrated solar power plants." *Engineering* 7.3 (2021): 334-347.

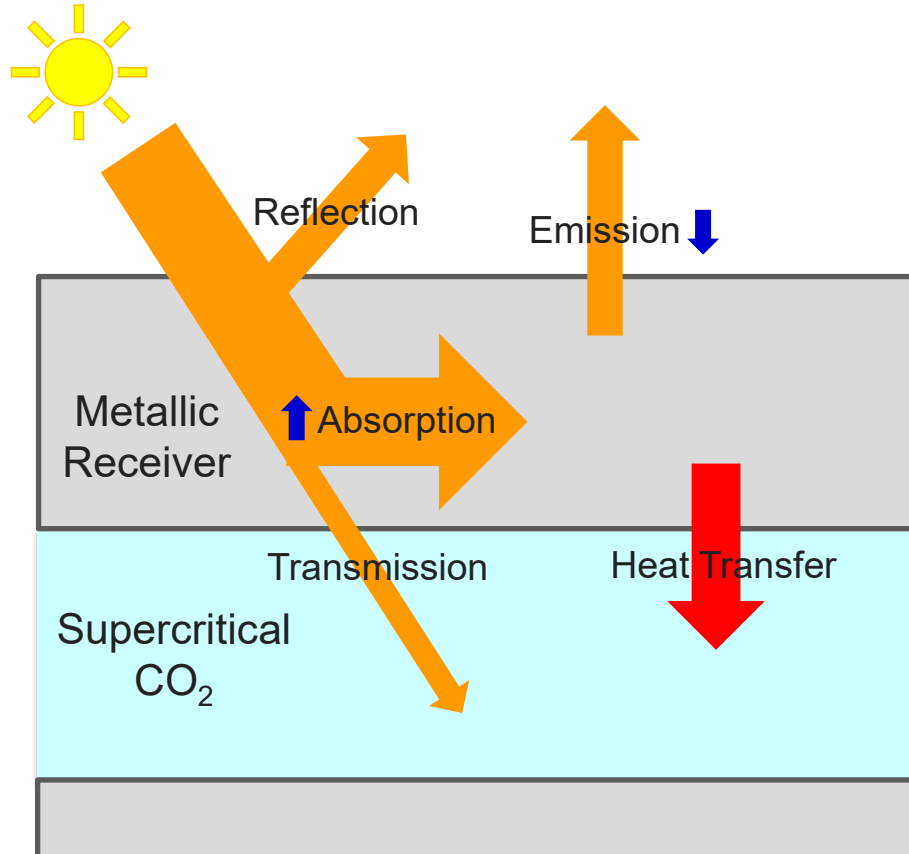


Sandia  
National  
Laboratories



Carnegie Mellon University

# Can we control the surface to increase the absorptivity?



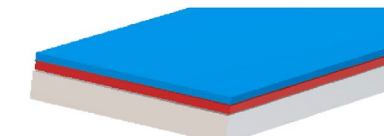
We want to maximize the absorptivity while minimizing the emissivity!

$$\text{Figure of Merit: } \eta = \frac{\alpha_{solar} Q - \varepsilon \sigma (T^4 - T_{surr}^4)}{Q}$$

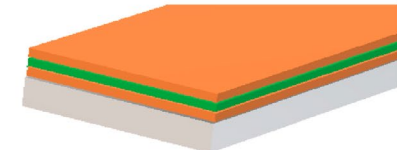
Intrinsic selective



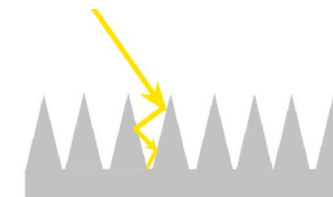
Semiconductor-metal tandems



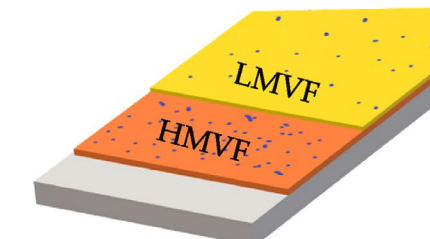
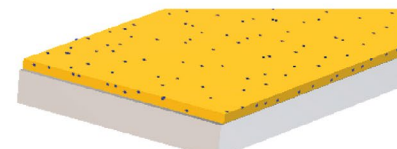
Multilayers



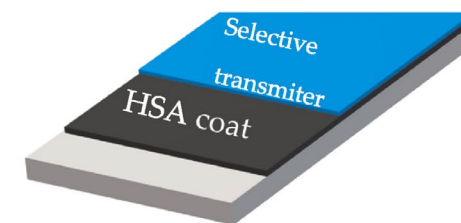
Textured surfaces



Cermet and double cermet



Selectively solar-transmitting coating on a blackbody-like absorber



Various ways to increase the absorptivity<sup>3</sup>

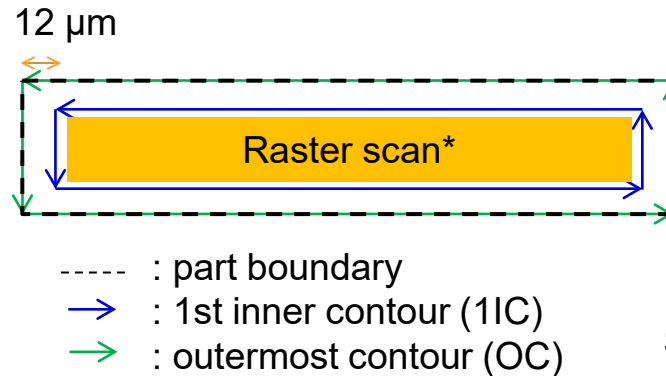
<sup>3</sup>Noč, Luka, and Ivan Jerman. "Review of the spectrally selective (CSP) absorber coatings, suitable for use in SHIP." Solar Energy Materials and Solar Cells 238 (2022): 111625.

Experiments

# CO-DESIGNING, PRINTING, AND TESTING



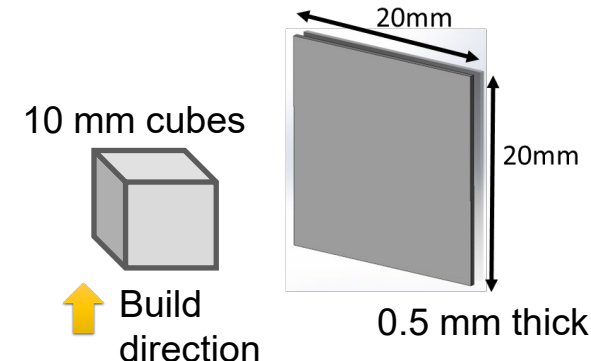
# Co-designing and printing



## Approach 1: Contour variation

Sample	Outermost contour parameter		1st inner contour parameter	
	P (W)	V (mm/s)	P (W)	V (mm/s)
SP9	80	800	138	390

Standard contour parameters (for  $L = 40 \mu\text{m}$ , Inconel 718, EOS M290)



Sample	Name	Outermost contour			1st inner contour
		P (W)	V (mm/s)	E density (J/mm <sup>2</sup> )	
CS10	Removed contour	OFF			
CS11	Reduce P 2-fold	40	800	1.25	
CS12	Increase P 2-fold	160	800	5	
CS13	Increase P 4-fold	320	800	10	
CS14	Reduce V 4-fold	80	200	10	OFF**
CS15	Reduce V 2-fold	80	400	5	
CS16	Increase V 2-fold	80	1600	1.25	
CS17	Max power	370	959	9.65	
CS18	Keyholing	370	350	26.4	
CS19	OC only	80	800	2.5	

Various contour parameters that were tried in this study

$$S_a = \frac{1}{A} \iint_A |Z(x, y)| \, dx \, dy$$

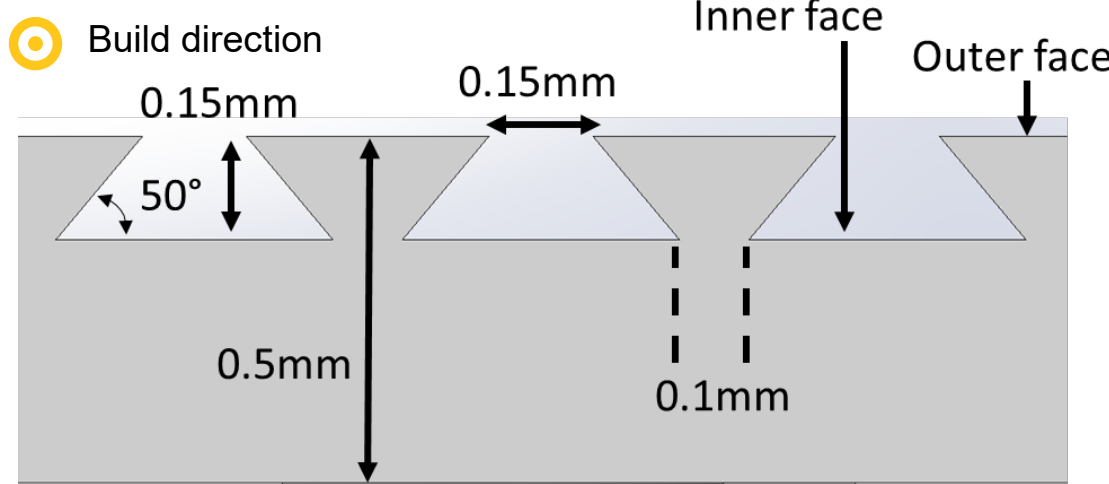
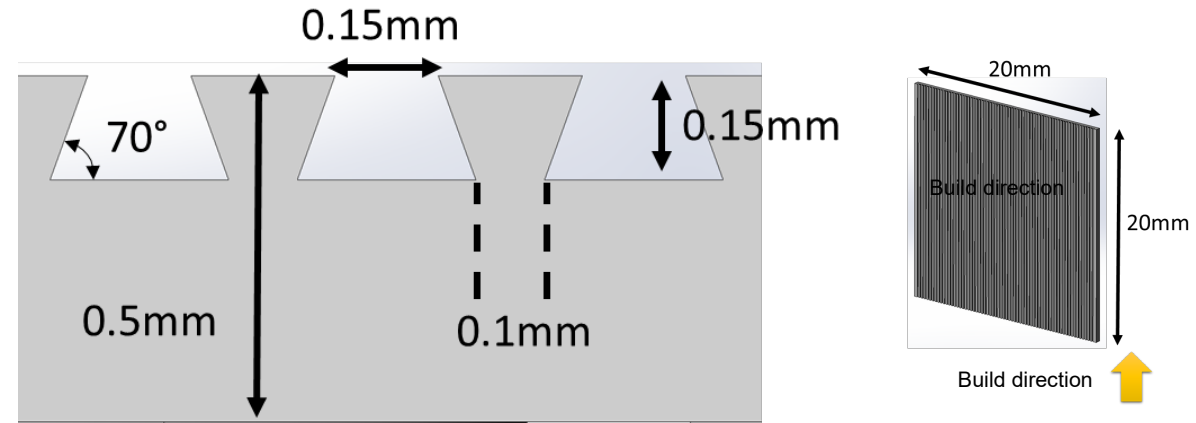
\* The infill parameters were kept constant throughout the study.

\*\* Our previous study of varying 1IC parameters showed that the most significant increase in the  $S_a$  happened in parts without 1IC.

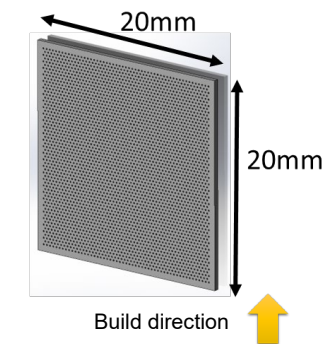
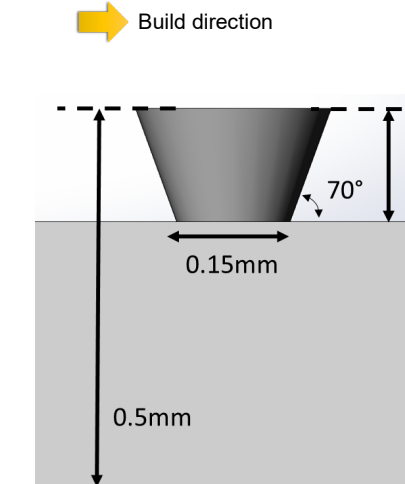
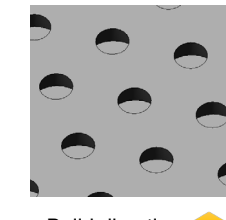
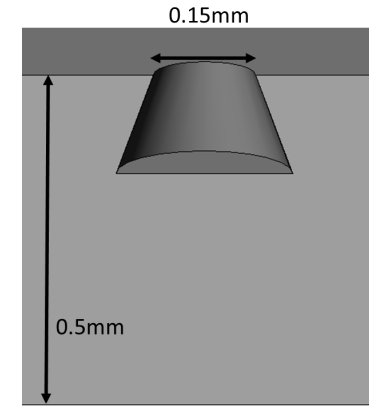
# Co-designing and printing

## Approach 2: CAD file variation

Vertical grooves



Divots and pegs



\* Standard infill and contour parameters were used to print the samples for approach 2.

**UCDAVIS**  
UNIVERSITY OF CALIFORNIA



# Surface evaluations

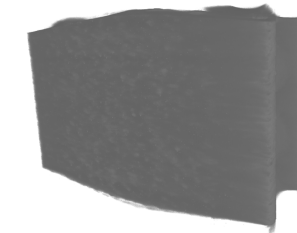
- Optical profilometry
  - Keyence VR-5000 Series

1. Reconstructs a height map.
  - Pixel size: 7.4  $\mu\text{m}$
2. Fast, wide-area scanning is possible.
  - $\frac{1}{2}$  hour to image a 20 mm by 20 mm surface.

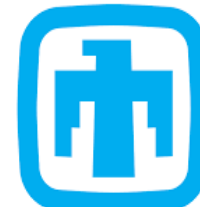
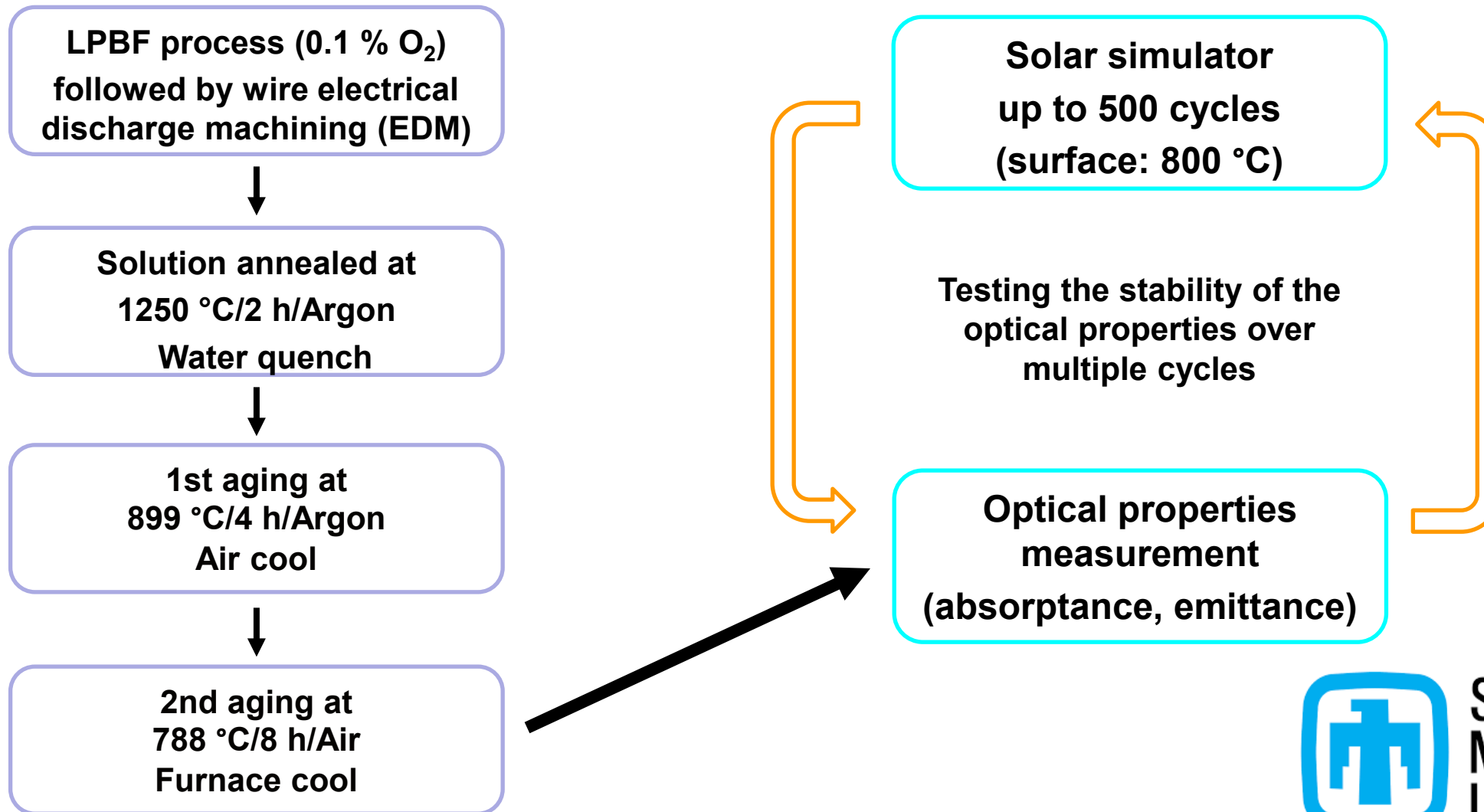


- Computed tomography
  - Zeiss Xradia CrystalCT

1. Reconstructs a point cloud.
  - Voxel size: 2.1  $\mu\text{m}$
2. Slow, but cavity features and porosity can be revealed.
  - 3 hours to image a 6 mm diameter 4 mm tall cylindrical region.
3. Voxel size and the field of view is limited by sample dimensions.



# Heat treatment and solar simulator testing



Sandia  
National  
Laboratories

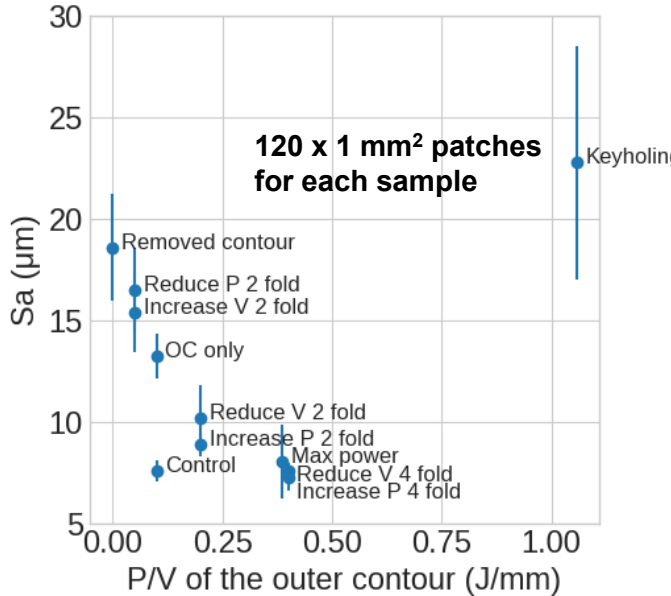
## Results and Discussion

# SURFACE AND OPTICAL PROPERTIES



The surface roughness measured using the optical profilometer

### Cubes



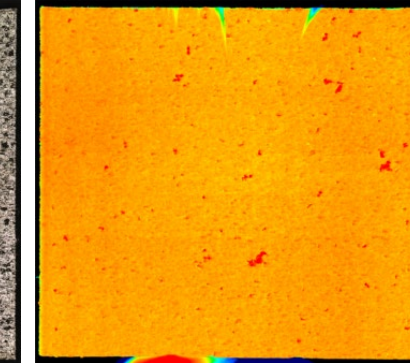
# Contour variations

- The addition of contour scans generally makes the surface smoother.
- The Sa surface roughness shows a U-shaped curve when plotted against the outer contour P/V. (most of the literature shows only an increasing or decreasing trend with respect to P/V)
- CS18 with keyholing contour parameters showed rather distinct discoloration on the surface.

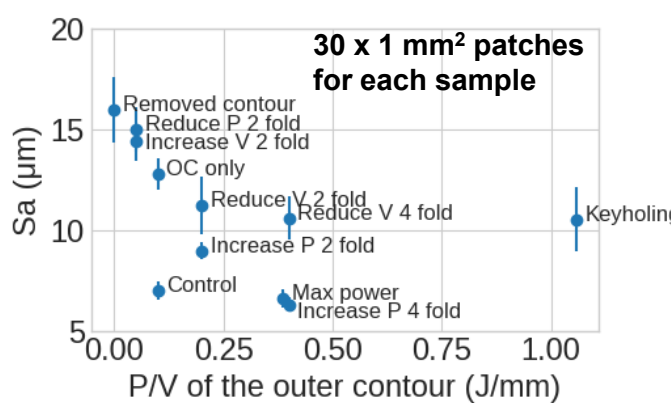
SP9 Control (Smooth baseline)



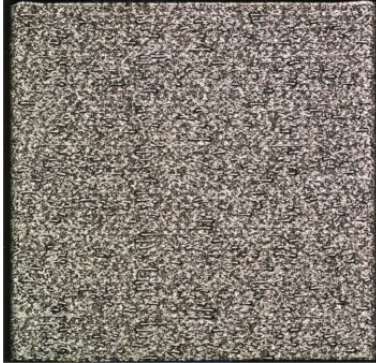
CS14 Reduce V 4-fold (Occasional bumps)



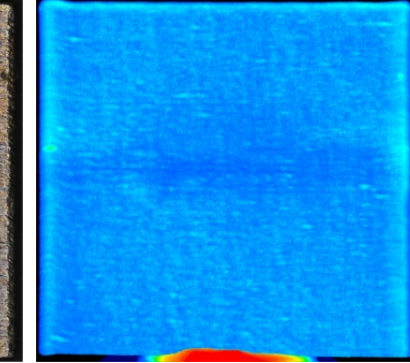
### Thin walls



CS10 Removed contour (Roughest)



CS18 Keyholing (Discoloration)

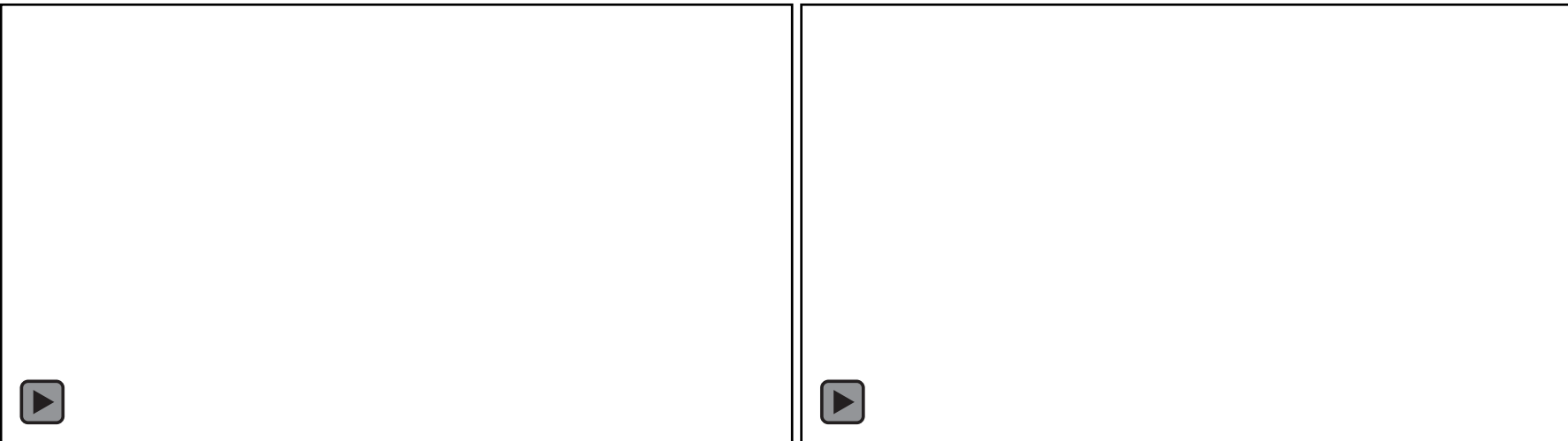


Build Direction

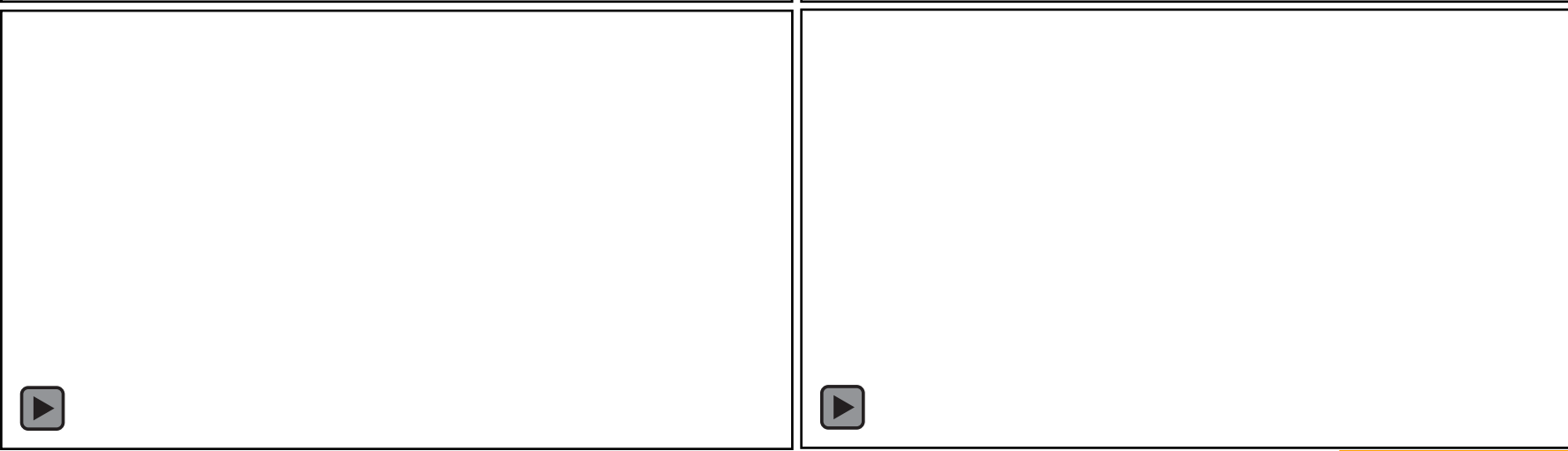
20 mm

# CAD files variations

- The surface features were printed, but the intended cavity structure was not achieved.



A group of spherical pores were observed around 300  $\mu\text{m}$  depth into the sample.



The samples suffered from cracks (moderate in SP-1, SP-2 and minor in SP-3, SP-4), which has never been observed in our bulk H282 parts printed with the same process parameters.

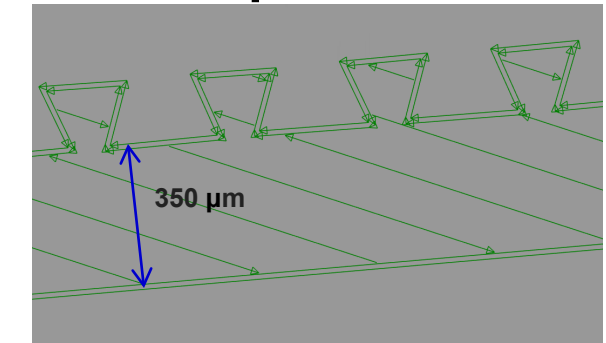
Bright region: metal, darker region: void

2 mm



# Why do we see the defects?

- The surface features were printed, but the intended cavity structure was not achieved.
  - This is suspected to be due to the melt pool being larger than the sharp corners. (The melt pool is larger in thin walls due to heat build-up.)
- A group of spherical pores were observed around 300  $\mu\text{m}$  depth into the sample.
  - This is suspected to be due to short melt pool turnarounds causing heat build-up. The identified pores look similar to keyhole porosity which is mainly due to excess energy input.
- The samples suffered from cracks (moderate in SP-1, SP-2 and rather minor in SP-3, SP-4) which has never been seen in our bulk H282 parts printed with the same process parameters.
  - We suspect there are a lot of variables of concern, such as residual stress. However, the complex patterning is responsible for the cracks since the thin walls without surface patterns did not show any cracks.



\* Chakraborty, Apratim, et al. "Micro-cracking mechanism of RENÉ 108 thin-wall components built by laser powder bed fusion additive manufacturing." *Materials Today Communications* 30 (2022): 103139.

\*\* Shahabad, Shahriar Imani, et al. "On the effect of thin-wall thickness on melt pool dimensions in laser powder-bed fusion of Hastelloy X: Numerical modeling and experimental validation." *Journal of Manufacturing Processes* 75 (2022): 435-449.



# Effects of the heat treatment

Images of the samples in crucible for the heat treatment

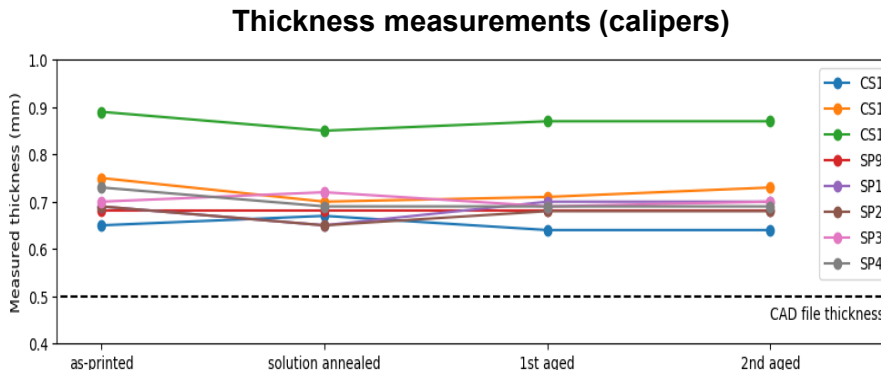


As-printed  
(0.1 %O<sub>2</sub>)

Solution annealed at  
1250 °C/2 h/Argon  
Water quench

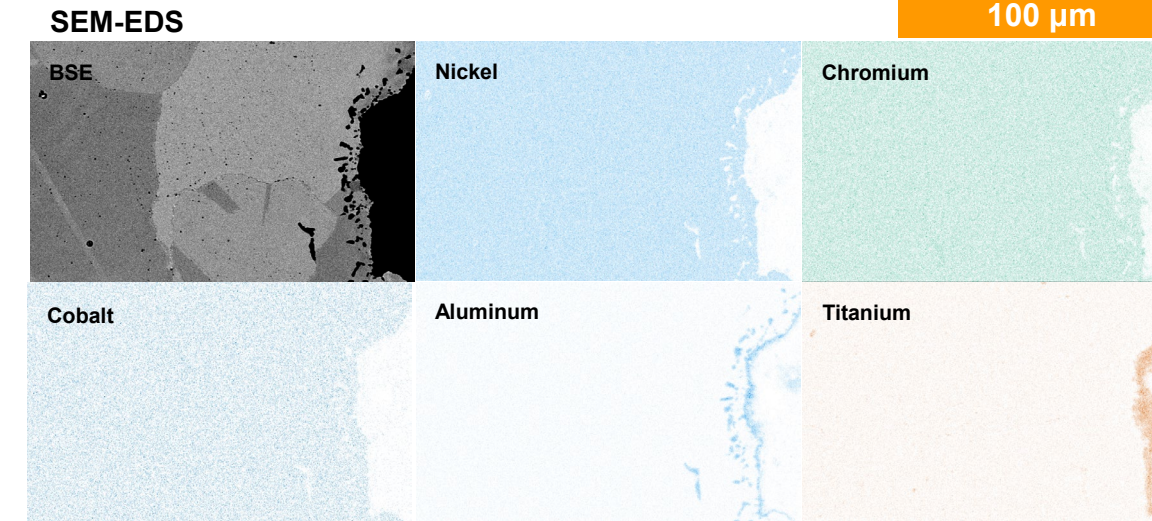
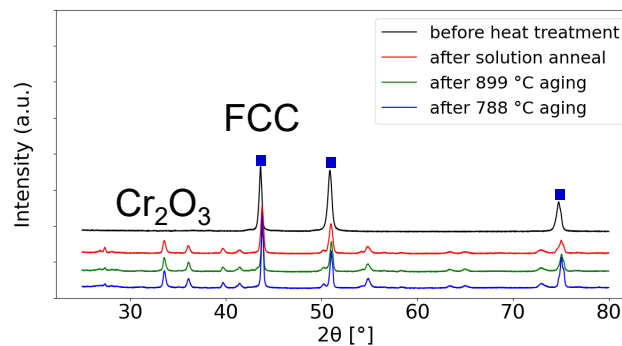
1st aged at  
899 °C/4 h/Argon  
Air cool

2nd aged at  
788 °C/8 h/Air  
Furnace cool



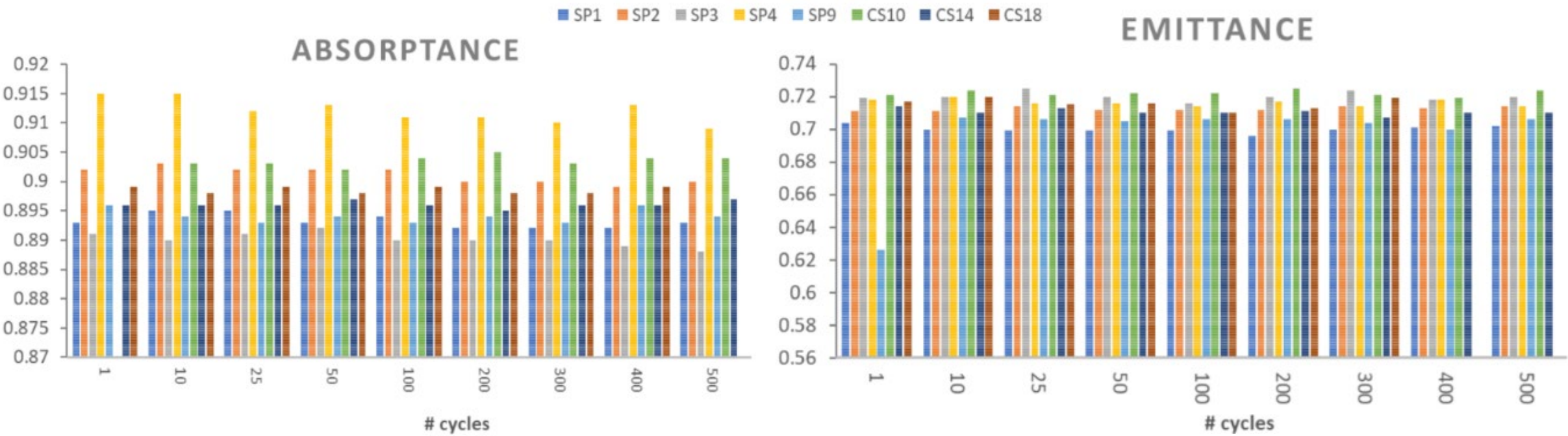
- Measuring the thickness with a caliper after each step did not show a significant trend (no severe oxide flake-off).
- CS18 (keyholing contour) and CS10 (contour removed) were the thickest and thinnest samples, respectively.

XRD measurements (surface 10  $\mu\text{m}$ )



- EDS measurements after the full heat treatment showed a layer of 10 ~ 15  $\mu\text{m}$  thick Al-and-Ti-rich oxide with occasional Al-rich oxide particles buried deeper (25 ~ 30  $\mu\text{m}$ ) into the bulk.
- The oxide layer giving the darkened surface improves absorptance.

# Absorptance & emittance measurements

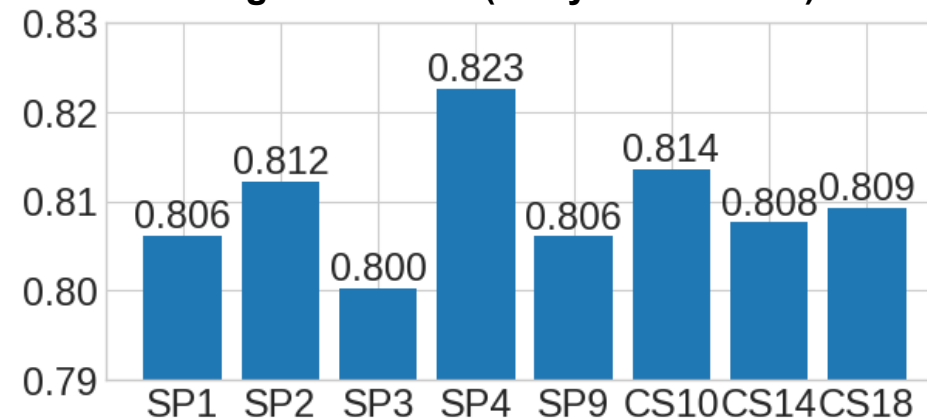


$$\eta = \frac{\alpha_{solar} Q - \varepsilon \sigma (T^4 - T_{surr}^4)}{Q}$$

$$\eta \cong \alpha_{solar} - \frac{\varepsilon}{8}$$

when  $T = 1073 \text{ K}$ ,  $T_{surr} = 293 \text{ K}$ ,  
 $\sigma = 5.67 * 10^{-12} \text{ W/cm} \cdot \text{K}^4$ ,  
 $Q = 60 \text{ W/cm}^2$  (600 suns)

Figure of merit (10 cycles onward)

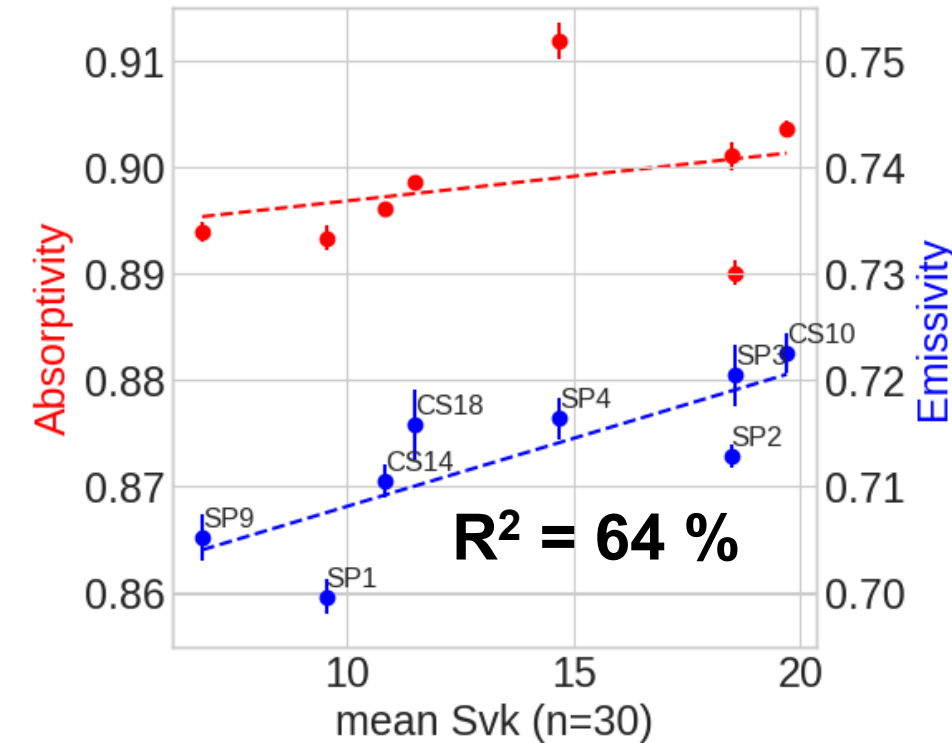
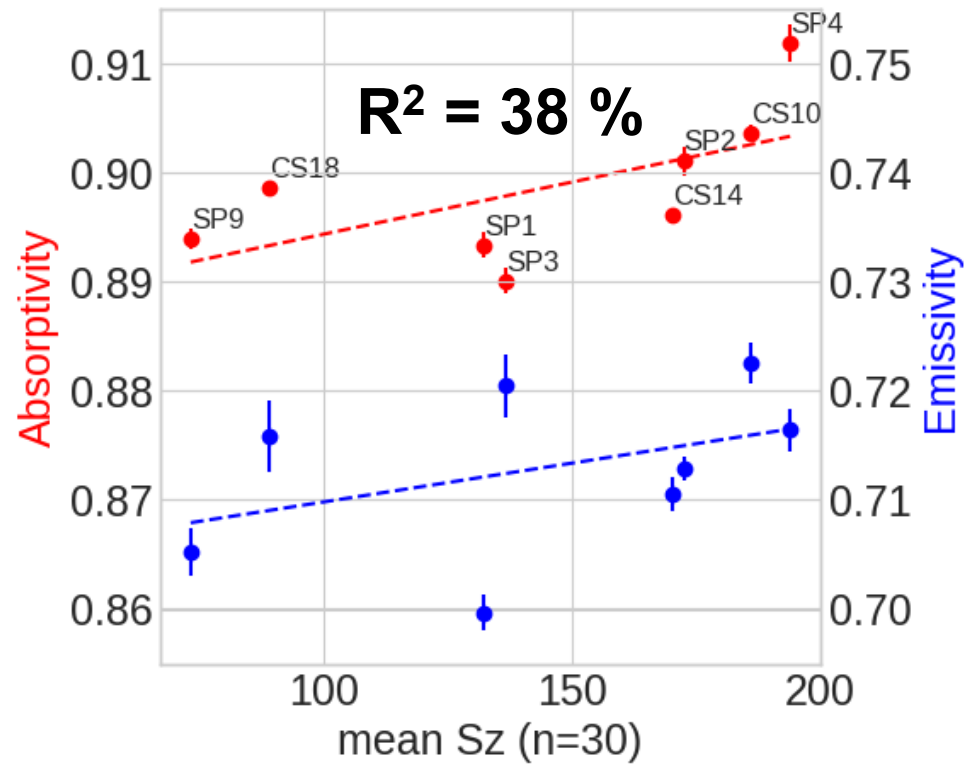


From 10 cycles onwards, the absorptance and emittance measurements stay relatively stable over cycles (advantages over some coatings techniques).

Over 500 cycles, SP-4 (pegs) has the best figure of merit followed by CS10 (contour removed) due to the high absorptance.



# Surface roughness vs optical properties



Surface roughness parameter  $S_z$  and  $S_{vk}$  seems to be a better predictor of absorptivity and the emissivity , respectively, than  $S_a$  or  $S_v$  for this dataset. An optical ray tracing study will follow to provide better insight.



# Conclusions & Future work

## Conclusions

1. We show cost-and-time-efficient ways of inducing surface patterns during printing to tailor the optical properties.
2. Addition of a contour parameter generally reduces the roughness, and there seems to be an optimal P/V ratio for printing smooth surfaces.
3. Although the surface patterned samples failed to achieve cavity structures, two of them (SP-2 and SP-4) showed an improved absorptance that led to a higher figure of merit than the baseline.

## Future work

1. The process will be modified to fabricate samples with better dimensional accuracy and density and further increase the figure of merit.
2. Additional experiments will follow to confirm our u-shaped process window in the surface roughness vs contour P/V space for thin walls and bulk cubes.
3. Optical ray tracing will be used to confirm that our surface patterns are causing the increase in absorptance.



# Acknowledgments

- This work is supported by EERE-SETO Award # DE-EE0010190.
- Parts of this work are supported by EERE-SETO Award # DE-EE0008536.
- Parts of this work are supported by ARPA-E Award # DE-AR0001127.
- The authors acknowledge use of the Materials Characterization Facility at CMU supported by grant MCF-677785.
- Sandia National Laboratories is a multimission laboratory managed and operated by National Technology & Engineering Solutions of Sandia, LLC, a wholly owned subsidiary of Honeywell International Inc., for the U.S. Department of Energy's National Nuclear Security Administration under contract DE-NA0003525.
- This work utilized the NextManufacturing Center facilities at CMU.
- Nicholas Lamprinakos, PJ Wilkerson, and Ian MacLachlan at CMU assisted with fabrication and machining and heat treatment of the samples.
- Dr. Ping Wang provided advice on the heat treatment of Haynes 282.
- Funding to attend this conference was provided by the CMU Graduate Student Assembly/Provost Conference Funding.

